

High-strength Ti-Al-V-Zr cast alloys designed using α and β cluster formulas

Zhi-hao Zhu¹, Yu-han Liu¹, Zhi-peng Chen¹, Tian-yu Liu², Shuang Zhang³, *Dan-dan Dong⁴, and Chuang Dong^{1,3}

1. Key Laboratory for Materials Modification by Laser, Ion, and Electron Beams and School of Materials Science and Engineering, Dalian University of Technology, Dalian 116024, Liaoning, China

2. State Key Laboratory of Light Alloy Casting Technology for High-end Equipment, Shenyang Research Institute of Foundry Co., Ltd., Shenyang 110022, China

3. School of Materials Science and Engineering, Dalian Jiaotong University, Dalian 116028, Liaoning, China

4. College of Physical Science and Technology, Dalian University, Dalian 116622, Liaoning, China

Abstract: Ti-Al-V-Zr quaternary titanium alloys were designed following α - $\{[\text{Al-Ti}_{12}](\text{AlTi}_2)\}_{17-n}+\beta$ - $\{[\text{Al-Ti}_{12}\text{Zr}_2](\text{V}_3)\}_n$, where $n=1-7$ (the number of β units), on the basis of the dual-cluster formula of popular Ti-6Al-4V alloy. Such an alloying strategy aims at strengthening the alloy via Zr and V co-alloying in the β -Ti unit, based on the original β formula $[\text{Al-Ti}_{14}](\text{V}_2\text{Ti})$ of Ti-6Al-4V alloy. The microstructures of the as-cast alloys by copper-mold suction-casting change from pure α ($n=1$) to $\alpha+\alpha'$ martensite ($n=7$). When n is 6, Ti-5.6Al-6.8V-8.1Zr alloy reaches the highest ultimate tensile strength of 1,293 MPa and yield strength of 1,097 MPa, at the expense of a low elongation of 2%, mainly due to the presence of a large amount of acicular α' martensite. Its specific strength far exceeds that of Ti-6Al-4V alloy by 35%.

Keywords: titanium alloy; cluster-plus-glue-atom model; composition design; microstructure; mechanical properties

CLC numbers: TG146.23

Document code: A

Article ID: 1672-6421(2023)01-023-06

1 Introduction

Ti-6Al-4V alloy with $\alpha+\beta$ dual-phase microstructure is the most popular Ti alloy due to its balanced mechanical properties^[1-3]. At as-cast state, its ultimate tensile strength (UTS) reaches 820–1,000 MPa and elongation reaches 4%–20%. To meet the stringent requirements of aerospace industry, the strength of the alloy needs to be further improved. High-strength β Ti alloy series such as β -21S, BT22, Ti-55531 and β -CEZ have been developed, whose UTS can reach beyond 1,300 MPa^[4]. However, the β Ti alloys suffer from an insufficient high-temperature structure stability and a poor machinability caused by strong β -stabilizers such as Mo, V, Cr, and Fe, which have high self-diffusivities and low thermal conductivities^[5]. Furthermore, typical high-temperature near- α Ti alloys, such as Ti1100, IMI834, and Ti60, show limited UTS below 1,200 MPa^[6]. Therefore, it is

urgent to find high-strength Ti alloys with UTS above 1,200 MPa.

Recently, based on the framework of the so-called "cluster-plus-glue-atom" model, a new structural tool for the description of solid solutions, the widely-used Ti-6Al-4V alloy composition is able to be interpreted via a dual-cluster formula α - $\{[\text{Al-Ti}_{12}](\text{AlTi}_2)\}_{12}+\beta$ - $\{[\text{Al-Ti}_{14}](\text{V}_2\text{Ti})\}_5$, where the two structural units in proportion 12:5 correspond respectively to α - and β -Ti phases^[7]. This formula provides the basis for the composition optimization of various Ti alloys: by varying the ratio of the α and β units and alloying them separately, different Ti alloys can be formulated, as exemplified in low-elastic-modulus biomedical β -Ti alloys^[8], additive manufactured $\alpha+\beta$ Ti alloys^[9,10], and high temperature near- α Ti alloys^[11].

The present work attempts to develop high-strength Ti alloys on the basis of the dual-cluster formula of Ti-6Al-4V alloy. It is noted that the Ti-6Al-4V alloyed with Zr shows increased strength, though still below 1,200 MPa^[12]. Therefore, Ti-Al-V-Zr quaternary alloys were designed following α - $\{[\text{Al-Ti}_{12}](\text{AlTi}_2)\}_{17-n}+\beta$ - $\{[\text{Al-Ti}_{12}\text{Zr}_2](\text{V}_3)\}_n$, where the number of β units, n , ranges from 1 to 7, and the β -Ti unit is further stabilized via Zr and V co-alloying, relative to the original β formula $[\text{Al-Ti}_{14}](\text{V}_2\text{Ti})$ of Ti-6Al-4V alloy. The alloys were prepared by

*Dan-dan Dong

Female, Ph.D., Dalian Young Star of Science and Technology. Her research interests mainly focus on the structural modeling and composition design of complex alloys, including metallic glasses, solid solutions, and lead-free solders.

E-mail: dandan3006@126.com

Received: 2022-05-18; Accepted: 2022-10-24

copper-mold suction casting. Their microstructure and mechanical properties at as-cast state were investigated.

2 Materials and methods

To design a high-strength alloy, two modifications were made to the 17-unit dual-cluster formula $\alpha\text{-}\{[\text{Al-Ti}_{12}](\text{AlTi}_2)\}_{12} + \beta\text{-}\{[\text{Al-Ti}_{14}](\text{V}_2\text{Ti})\}_5$ of Ti-6Al-4V alloy. First, the initial β -unit $[\text{Al-Ti}_{14}]\text{V}_2\text{Ti}$ of Ti-6Al-4V alloy was transformed to $[\text{Al-Ti}_{12}\text{Zr}_2](\text{V}_3)$ by Zr and V co-alloying to enhance the β structural stability. The Ti-Zr system forms a completely solid solution for both β -phase (BCC structure) and α -phase (HCP structure)^[7]. Although Zr is generally considered as a neutral element, recent studies have found that β -phase content increases with increasing the Zr content^[12-13]. Element Zr shows a zero enthalpy of mixing with Ti^[14]. Therefore, Zr replaces Ti in the shell position in the β -Ti unit. Element V takes the glue site in the β unit, and the maximum β stability corresponds to the full occupation of the three glue sites. The ratio of Ti and Zr was chosen as 12:2 in the β unit on the basis of interpreting the formula of industrially widely used Zr-containing Ti60, IMI834, and Ti1100 alloys, as already done in Ref. [10], where the integer ratios of Ti to Zr fall close to 12:2 in the β unit. Second, the number of β units was varied following $\alpha\text{-}\{[\text{Al-Ti}_{12}](\text{AlTi}_2)\}_{17-n} + \beta\text{-}\{[\text{Al-Ti}_{12}\text{Zr}_2](\text{V}_3)\}_n$, $n=1-7$, or Ti-(5.3-7.1)Al-(1.2-7.8)V-(1.6-9.3)Zr (wt.%) formulas. The designed compositions are listed in Table 1.

To further clarify the designed compositions with respect to the reference Ti-6Al-4V alloy, the quaternary compositions are shown in a ternary composition diagram (Ti, Zr)-Al-V, as shown in Fig. 1. The designed compositions spread precisely along a straight line (red line) linking the stable $\alpha\text{-Al}_2\text{Ti}_{14}$ formula and a stable $\beta\text{-Al}_1(\text{Ti, Zr})_{14}\text{V}_3$ formula. In contrary, the reference alloy Ti-6Al-4V is located between $\alpha\text{-Al}_2\text{Ti}_{14}$ and another $\beta\text{-Al}_1\text{Ti}_{15}\text{V}_2$ formula. Multiple β formulas are possible, whose positions are marked by open circles. The corresponding Mo- and Al-equivalents fall respectively in ranges 0.8wt.%-5.2wt.% and

Table 1: Compositions and equivalents of designed alloys and Ti-6Al-4V reference alloy

Material code	n	Composition (wt.%)	$[\text{Mo}]_{\text{eq}}$ (wt.%)	$[\text{Al}]_{\text{eq}}$ (wt.%)
$n1$	1	Ti-7.1Al-1.2V-1.6Zr	0.8	7.4
$n2$	2	Ti-6.8Al-2.4V-2.9Zr	1.6	7.3
$n3$	3	Ti-6.5Al-3.5V-4.2Zr	2.4	7.2
$n4$	4	Ti-6.2Al-4.6V-5.6Zr	3.1	7.1
$n5$	5	Ti-5.9Al-5.7V-6.8Zr	3.8	7.0
$n6$	6	Ti-5.6Al-6.8V-8.1Zr	4.5	6.9
$n7$	7	Ti-5.3Al-7.8V-9.3Zr	5.2	6.8
Ti-6Al-4V	-	Ti-6.05Al-3.94V	2.6	6.1

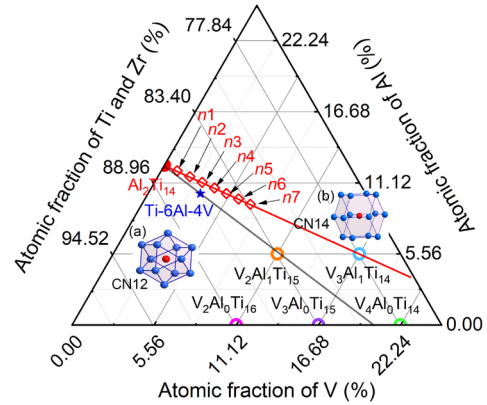


Fig. 1: (Ti, Zr)-Al-V pseudo-ternary composition diagram showing positions of designed compositions (red open squares) extending along a straight red line linking $\alpha\text{-Al}_2\text{Ti}_{14}$ formula and $\beta\text{-Al}_1\text{Ti}_{14}\text{V}_3$ formula. The clusters of α - and β -Ti, twinned cuboctahedron (a) and rhombic dodecahedron (b), are also shown

6.8wt.%-7.4wt.%, using the expressions $[\text{Mo}]_{\text{eq}} = 1.0\text{Mo} + 1/3.6\text{Nb} + 1/4.5\text{Ta} + 1/2\text{W} + 1/0.63\text{Cr} + 1/0.65\text{Mn} + 1/1.5\text{V} + 1/0.35\text{Fe} + 1/0.8\text{Ni}$ ^[15] and $[\text{Al}]_{\text{eq}} = 1.0\text{Al} + 1/3\text{Sn} + 1/6\text{Zr} + 100$ ^[16].

3 Experimental procedure

The alloys were prepared via copper-mold arc melting. Pure Ti (99.9%), Al (99.99%), V (99.99%) and Zr (99.5%) were melted in a vacuum arc melting furnace under argon protective atmosphere. After melting five times to ensure composition uniformity, the melt was suction-cast into a bar-shaped copper-mold of 60 mm in length and 6 mm in diameter. The ingots are shown in Fig. 2(a).

The microstructures were investigated by scanning electron microscopy (SEM, Zeiss Supra 55) and X-ray diffraction (XRD, XRD-6000) using Cu-K α radiation with a scan rate of 4°·min⁻¹. Tensile tests were performed on a UTM5504-G electronic universal test machine at a rate of 0.25 mm·min⁻¹ at ambient temperature. Dog-bone-shaped specimens for tensile tests were 15 mm in gauge length and 3 mm in diameter, as shown in Fig. 2(b). Three tensile tests were conducted for each alloy. The mass density was investigated using a XS64 densimeter tester, where each alloy was measured at least three times.

4 Results and discussion

Figures 3(a-g) show the secondary electron images of as-cast Ti-Al-V-Zr alloys. As n increases from 1 to 7, the microstructure of the alloy changes from single α phase to $\alpha + \alpha'$ martensite. The morphology of α' martensite gradually changes from plate-like to lamellar, and finally to needle-like. Similar plate-like α' martensite in low-alloyed Ti alloys and needle-like α' martensite in high-alloyed ones were also reported in as-cast Ti-V-(Al, Sn) alloys quenched in ice water^[17]. The $n1$ alloy contains a single α phase. Lamellar α' martensite structure starts to appear in the $n2$ alloy. When n is 6, acicular α' martensite dominates in the matrix of Ti-5.6Al-6.8V-8.1Zr alloy. The reference Ti-6Al-4V

alloy is composed of α +lamellar α' martensite+a small amount of β phase, as shown in the arrow in Fig. 3(h). The increase of Zr content promotes the formation of α' martensite due to the effect of a solute-induced decrease in the martensite transformation start (M_s) point of α' martensite^[18]. Jing et al.^[12] also reported that in Ti-6Al-4V-xZr alloys, with increasing Zr content, α -phase platelets are replaced by a lamellar α' martensite phase, and the thickness of the lamellar α' martensite gradually decreases. When Zr or Ti alloys suffer rapid cooling from the two-phase or β -phase temperature region, the α' martensite is more likely to appear with the increasing β -phase stability^[19]. Therefore, in this study, the gradual increase of α' martensite with increasing Zr content can also be attributed to the decrease in the M_s point of α' martensite.

In the XRD spectra shown in Fig. 4(a), only α -Ti (α' martensite) diffraction peaks are observed. The peaks of the α' martensite gradually increase when n is small (from 1 to 3). This is mainly because a more stabilized β -phase is retained via V and Zr co-alloying after the rapid suction-casting process. Similar results were also reported in a Ti-6Al-4V-($x=5, 10, 15, 20$)Zr alloy^[12]. Figure 4(b) shows unit cell volume versus Mo-equivalent of the alloys. It is evident that the unit cell volumes of all the designed Ti-Al-V-Zr alloys are smaller than those of pure β -Ti and α -Ti. Joseph et al.^[20] reported that a smaller unit cell volume gives a lower internal stress of the crystal, which is beneficial to improving the microstructure stability of the material. Thus, the smaller unit cell volumes of the Ti-Al-V-Zr quaternary alloy series confirm a more stabilized β -phase by V and Zr co-alloying and a relatively stabilized α -phase by Al alloying. As shown in

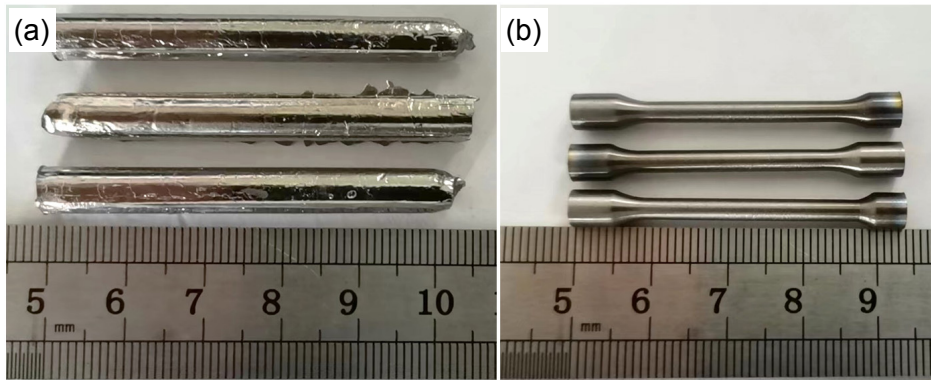


Fig. 2: Macrographs of copper-mold suction-casting bars (a) and dog-bone-shaped tensile specimens (b)

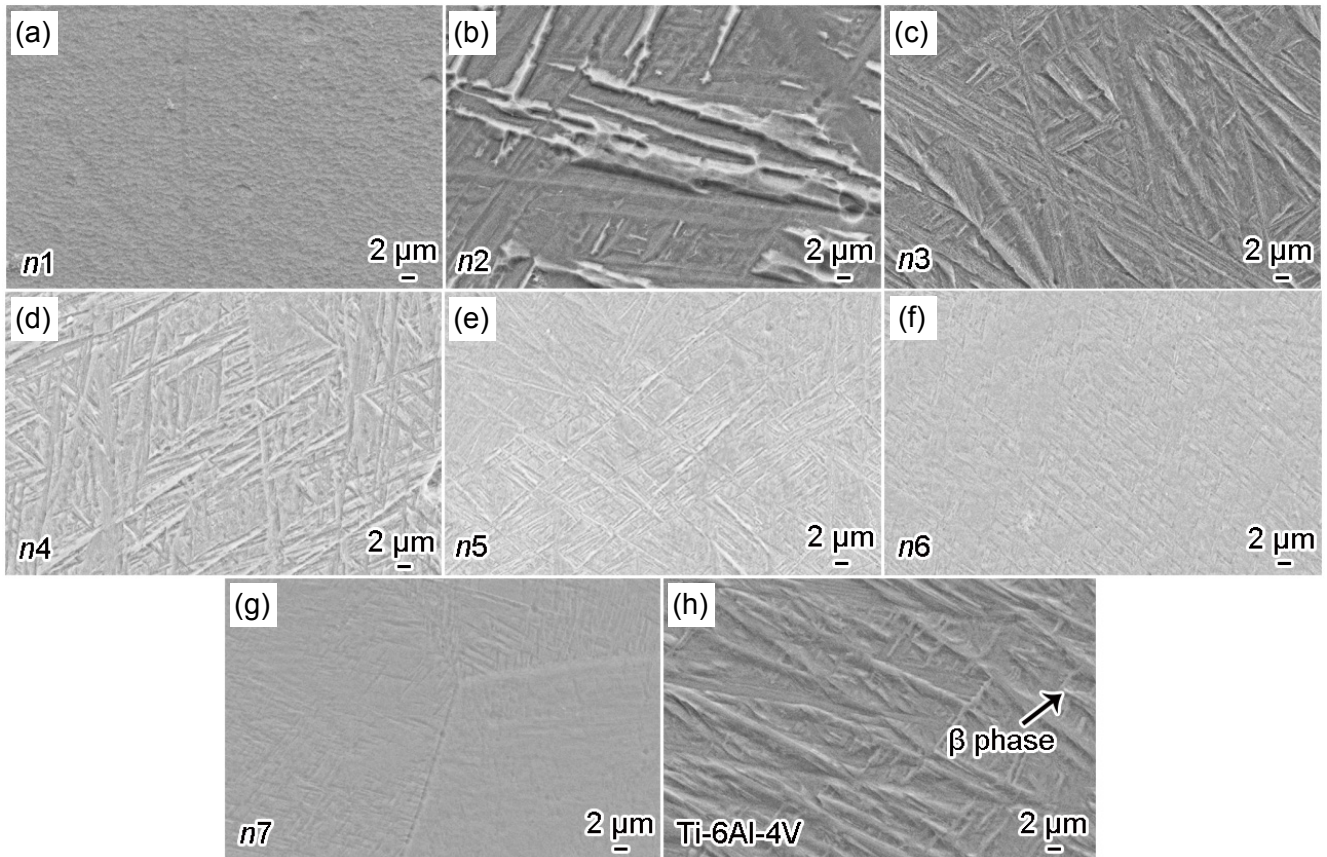


Fig. 3: SEM images of as-cast Ti-Al-V-Zr alloys with different n values

Fig. 4(b), the unit cell volumes of the designed alloys increase firstly and then decrease, and finally increase significantly with increasing n values (the number of β units, which also indirectly reflects the size of Mo-equivalent values). When n is 6, it is obvious that the unit cell volume of the Ti-5.6Al-6.8V-8.1Zr alloy is the smallest, about 0.0227 nm^3 , far smaller than 0.0235 nm^3 of the reference Ti-6Al-4V alloy. All the above microstructural changes suggest a better microstructural stability and therefore a high strength level for Ti-5.6Al-6.8V-8.1Zr alloy.

Figure 5(a) presents engineering stress-strain curves of the as-cast Ti-Al-V-Zr alloys. Yield strength (YS), ultimate tensile

strength (UTS) and elongation to failure (EL) are summarized in Fig. 5(b). As n increases, the strength increases at first and then decreases, while the plasticity changes inversely. The $n6$ alloy shows the highest UTS of 1,293 MPa and YS of 1,097 MPa, and the lowest elongation of 2%. Particularly, its strength is 1.4 times the reference Ti-6Al-4V alloy. In fact, the UTS of $n6$ alloy is higher than any of the reported (Ti, Zr)-6Al-4V quaternary alloys [12] and all popular high-temperature near- α Ti alloys [6]. It is even close to those of typical high-strength metastable β Ti alloys [4]. The improvement in strength is mainly related to the combination effects of solid solution

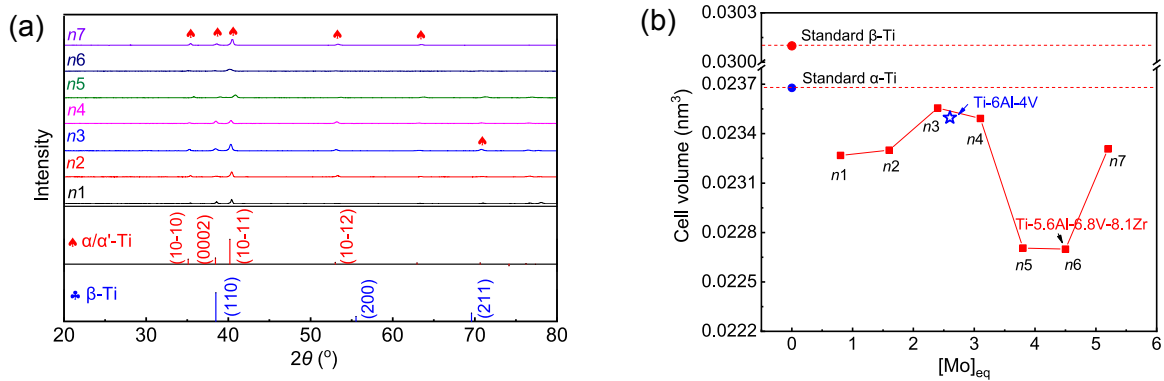


Fig. 4: XRD spectra (a), and unit cell volume vs. Mo-equivalent (b) of as-cast Ti-Al-V-Zr alloys. The unit cell parameters were collected from XRD spectra in (a)

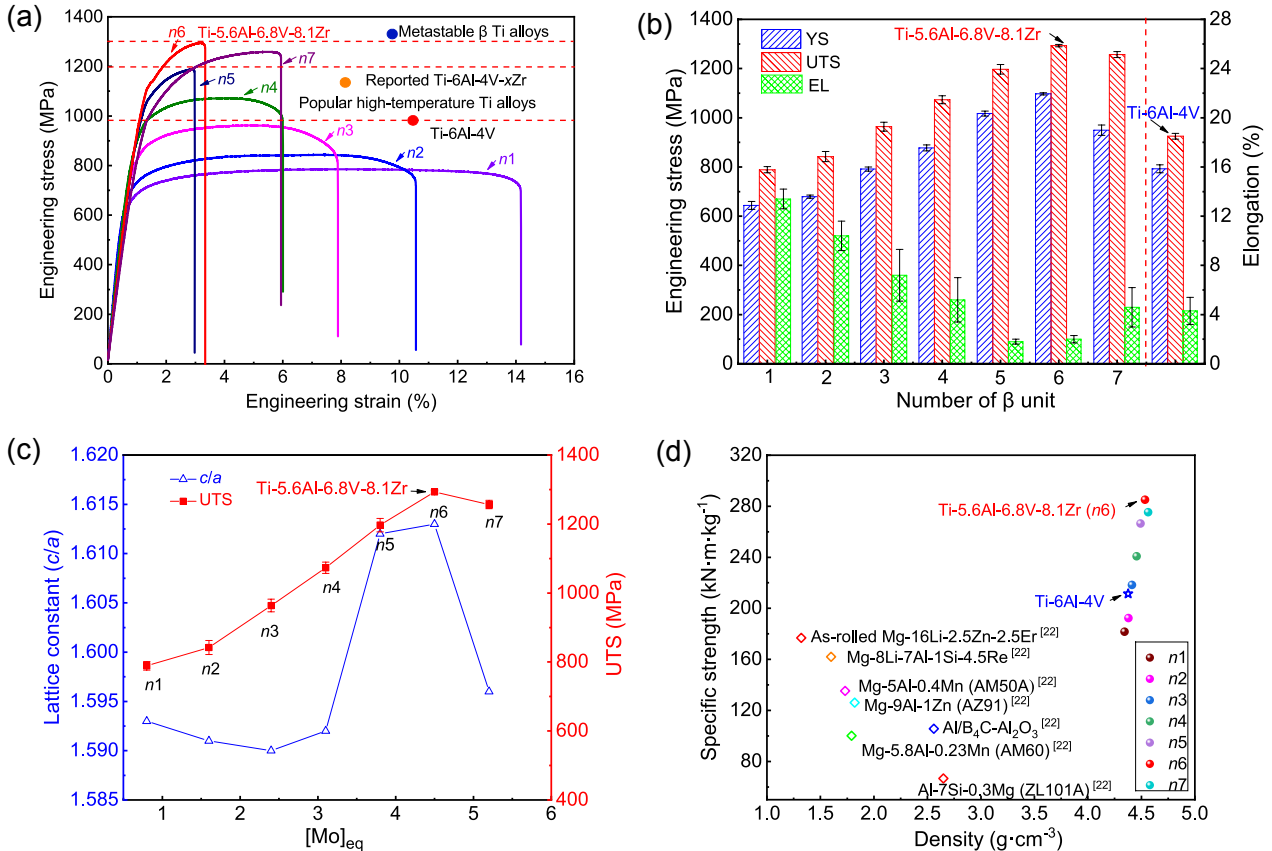


Fig. 5: Engineering strain-stress curves (a), YS, UTS and EL (b), lattice constant (c) and comparison of specific strengths (d) of Ti-Al-V-Zr as-cast alloys with some conventional light-weight alloys [22]. The red dotted lines in (a) respectively denote the reported UTS of Ti-6Al-4V-(5, 10, 15, 20) Zr alloys [12], popular high-temperature near- α Ti alloys [6], and typical high-strength metastable β Ti alloys [4]

strengthening and second phase (α' martensite) strengthening^[12]. The lattice constants (c and a) and c/a ratios of the alloys are listed in Table 2. It is noted that individual c and a do not show clear dependence on alloy composition but c/a varies linearly, as shown in Fig. 5(c). This is consistent with the results reported by Kawabata et al.^[21] that the strength of Ti alloy increases with the increase of c/a . Among the designed alloys, the $n6$ alloy shows the highest c/a ratio of 1.613, even much higher than the 1.593 of the reference Ti-6Al-4V alloy, indicating a better solid solution strengthening. Furthermore, a great amount of fine

acicular α' martensite is formed in the $n6$ alloy, as shown in Fig. 3(f). Such a fine acicular α' martensite inhibits dislocation movement and enhances the strength of alloys^[12]. When n is 1, the single- α $n1$ alloy shows the highest elongation, about 14%, three times that of the Ti-6Al-4V alloy, as shown in Fig. 5(b). This is due to the fact that the $n1$ alloy shows a single- α solid solution structure, as shown in Fig. 3(a), resulting in that the plastic deformation occurs more easily than that of the reference Ti-6Al-4V alloy.

Table 2: Lattice constants of the designed alloys and reference Ti-6Al-4V alloy

Material code	Composition (wt.%)	Lattice constants		
		c	a	c/a
$n1$	Ti-7.1Al-1.2V-1.6Zr	4.668	2.930	1.593
$n2$	Ti-6.8Al-2.4V-2.9Zr	4.668	2.932	1.592
$n3$	Ti-6.5Al-3.5V-4.2Zr	4.681	2.944	1.590
$n4$	Ti-6.2Al-4.6V-5.6Zr	4.681	2.940	1.592
$n5$	Ti-5.9Al-5.7V-6.8Zr	4.666	2.895	1.612
$n6$	Ti-5.6Al-6.8V-8.1Zr	4.668	2.894	1.613
$n7$	Ti-5.3Al-7.8V-9.3Zr	4.676	2.931	1.595
Ti-6Al-4V	Ti-6.05Al-3.94V	4.682	2.939	1.593

The average density data of the alloys are reported in Fig. 5(d). The $n6$ alloy exhibits the highest specific strength (UTS over mass density) of $285 \text{ kN}\cdot\text{m}\cdot\text{kg}^{-1}$, which is increased by 35% compared with the reference Ti-6Al-4V alloy of $211 \text{ kN}\cdot\text{m}\cdot\text{kg}^{-1}$. In fact, the specific strengths of all designed Ti-Al-V-Zr cast alloys are superior to the conventional lightweight alloys, especially the $n6$ alloy: increased by 126% compared to $126 \text{ kN}\cdot\text{m}\cdot\text{kg}^{-1}$ of the popular AZ91 magnesium alloy, and even increased by 325% compared to $67 \text{ kN}\cdot\text{m}\cdot\text{kg}^{-1}$ of the widely used ZL101A aluminum alloy^[22], also shown in Fig. 5(d). Overall, the results show that the cluster formula approach, a new method for the composition design, can effectively realize the development of high-performance Ti alloys. At present, the $n6$ alloy designed using α and β cluster formulas shows an excellent tensile strength and specific strength, which has great potential as a candidate material for aerospace applications.

5 Conclusion

High-strength Ti-(5.3–7.1)Al-(1.2–7.8)V-(1.6–9.3)Zr (wt.%) alloys were designed following α - $\{[\text{Al-Ti}_{12}](\text{AlTi}_2)\}_{17-n} + \beta$ - $\{[\text{Al-Ti}_{12}\text{Zr}_2](\text{V}_3)\}_n$, where $n=1-7$ (the number of β units), based on the dual-cluster formula of popular Ti-6Al-4V alloy. These quaternary alloy series feature enhanced β stability

by Zr and V co-alloying in the β -Ti unit compared to the original β formula $[\text{Al-Ti}_{14}](\text{V}_2\text{Ti})$ of Ti-6Al-4V alloy. The microstructures of as-cast alloys by copper-mold suction-casting change from pure α ($n=1$) to $\alpha+\alpha'$ martensite ($n=7$). When n is 6, the Ti-5.6Al-6.8V-8.1Zr alloy reaches the highest ultimate tensile strength of 1,293 MPa and yield strength of 1,097 MPa, close to the typical high-strength metastable β Ti alloys, at the expense of a low elongation of 2%, mainly due to the presence of a large amount of acicular α' martensite. Its specific strength exceeds that of Ti-6Al-4V alloy by 35% and is far better than conventional light-weight alloys such as AZ91 magnesium alloy, Mg-Re alloys, ZL101A aluminum alloy and Al/B₄C-Al₂O₃ aluminum matrix composite.

Acknowledgements

This work was financially supported by the Key Discipline and Major Project of Dalian Science and Technology Innovation Foundation (Grant No. 2020JJ25CY004), and the National Basic Research Program of China (Grant No. 2020JCJQZD165).

Conflict of interest

The authors declare that they have no conflict of interest.

References

- [1] Banerjee D, Williams J C. Perspectives on titanium science and technology. *Acta Materialia*, 2013, 61(3): 844–879.
- [2] Zhang T L, Zhu J M, Yang T, et al. A new $\alpha+\beta$ Ti-alloy with refined microstructures and enhanced mechanical properties in the as-cast state. *Scripta Materialia*, 2022, 207(15): 114260.
- [3] Liu T Y, Liu H Y, Yao Q, et al. Microstructure and mechanical properties of laser additive manufactured novel titanium alloy after heat treatment. *China Foundry*, 2021, 18(6): 574–580.
- [4] Ivasishin O M, Markovsky P E, Matviychuk Y V, et al. A comparative study of the mechanical properties of high-strength β -titanium alloys. *Journal of Alloys and Compounds*, 2008, 457: 296–309.
- [5] Cen M J, Liu Y, Chen X. Inclusions in melting process of titanium and titanium alloys. *China Foundry*, 2019, 18(4): 223–231.
- [6] Guo J L, Tian Y W. Research and development of 600 °C high temperature titanium alloys. *Foundry Technology*, 2020, 41: 894–896. (In Chinese)
- [7] Liu T Y, Zhang S, Wang Q, et al. Composition formulas of Ti alloys derived by interpreting Ti-6Al-4V. *Science China Technological Sciences*, 2021, 64: 1732–1740.
- [8] Wang Q, Ji C J, Wang Y M, et al. β -Ti Alloys with low Young's moduli interpreted by cluster-plus-glue-atom model. *Metallurgical and Materials Transactions A*, 2013, 44: 1872–1879.
- [9] Liu T Y, Zhu Z H, Zhang S, et al. Design for Ti-Al-V-Mo-Nb alloys for laser additive manufacturing based on a cluster model and on their microstructure and properties. *China Foundry*, 2021, 18(4): 424–432.
- [10] Zhu Z H, Liu T Y, Dong C, et al. Achieving high-temperature strength and plasticity in near- α Ti-7Al-3Zr-2V alloy using cluster formula design. *Journal of Materials Research and Technology*, 2022, 18: 2582–2592.
- [11] Che J D, Jiang B B, Wang Q, et al. Effects of minor Hf/Ta/Nb additions on high-temperature oxidation-resistant properties of near α -Ti alloys. *Transactions of Nonferrous Metals Society of China*, 2016, 26: 2086–2092. (In Chinese)
- [12] Jing R, Liang S X, Liu C Y, et al. Structure and mechanical properties of Ti-6Al-4V alloy after zirconium addition. *Materials Science and Engineering: A*, 2012, 552: 295–300.
- [13] Dobromyslov A V, Elkin V A. Martensitic transformation and metastable β -phase in binary titanium alloys with d-metals of 4–6 periods. *Scripta Materialia*, 2001, 44: 905–910.
- [14] Takeuchi A, Inoue A. Classification of bulk metallic glasses by atomic size difference, heat of mixing and period of constituent elements and its application to characterization of the main alloying element. *Materials Transactions*, 2005, 46: 2817–2829.
- [15] Mehjabeen A, Xu W, Qiu D, et al. Redefining the β -phase stability in Ti-Nb-Zr alloys for alloy design and microstructural prediction. *Powder Metallurgy of Non-Ferrous Metals*, 2018, 70: 2254–2259.
- [16] Kitashima T, Suresh K S, Yamabe-Mitarai Y. Effect of germanium and silicon additions on the mechanical properties of a near- α titanium alloy. *Materials Science and Engineering: A*, 2014, 579: 212–218.
- [17] Matsumoto H, Yoneda H, Fabregue D, et al. Mechanical behaviors of Ti-V-(Al, Sn) alloys with α' martensite microstructure. *Journal of Alloys and Compounds*, 2011, 509: 2684–2692.
- [18] Ho W F, Chen W K, Wu S C, et al. Structure, mechanical properties, and grindability of dental Ti-Zr alloys. *Journal of Materials Science: Materials in Medicine*, 2008, 19: 3179–3186.
- [19] Liang S X, Ma M Z, Jing R, et al. Preparation of the ZrTiAlV alloy with ultra-high strength and good ductility. *Materials Science and Engineering: A*, 2012, 539: 42–47.
- [20] Joseph M, Varghese S, Nicholas M H. First-principles calculations of the phase stability of TiO₂. *Physical Review B*, 2002, 65: 224112.
- [21] Kawabata T, Tamura T, Izumi O. Effect of Ti/Al ratio and Cr, Nb, and Hf additions on material factors and mechanical properties in TiAl. *Metallurgical Transactions A*, 1993, 24: 141–150.
- [22] Ji Q, Wang Y, Wu R Z, et al. High specific strength Mg-Li-Zn-Er alloy processed by multi deformation processes. *Materials Characterization*, 2020, 160: 110135.